Journal of Alloys and Compounds 509 (2011) 4520–4524

Contents lists available at ScienceDirect

Journal of Alloys and Compounds

journal homepage: www.elsevier.com/locate/jallcom

Structural, optical and hydrophilic properties of nanocrystalline TiO_2 ultra-thin films prepared by pulsed dc reactive magnetron sputtering

M. Horprathum[a,*], P. Eiamchai[a], P. Limnonthakul[d], N. Nuntawong[a], P. Chindaudom[a], A. Pokaipisit[b,c], P. Limsuwan[b,c]

[a] Optical Thin-Film Laboratory, National Electronics and Computer Technology Center, Pathumthani 12120, Thailand
[b] Department of Physics, Faculty of Science, King Mongkut's University of Technology Thonburi, Bangkok 10140, Thailand
[c] Thailand Center of Excellence in Physics, CHE, Ministry of Education, Bangkok 10400, Thailand
[d] Department of Physics, Faculty of Science, Srinakharinwirot University, Bangkok 10110, Thailand

ARTICLE INFO

Article history:
Received 26 February 2009
Received in revised form 7 January 2011
Accepted 8 January 2011
Available online 16 January 2011

PACS:
61.05.cp
68.37.Ps
81.15.Cd
82.30.Rs

Keywords:
Optical properties
Photo-induced hydrophilic
Sputtering
Thin films
Titanium dioxide

ABSTRACT

TiO_2 ultra-thin (15 nm) films were deposited on silicon wafers (100) and glass slides by pulsed dc reactive magnetron sputtering in an ultra-high vacuum (UHV) system. The effects of substrate temperature, from room temperature to 400 °C, on structural, optical, and hydrophilic properties of the obtained films have been investigated. The structure of the films was characterized by grazing-incidence X-ray diffraction, high-resolution transmission electron microscopy, and atomic force microscopy. The optical properties were determined by UV–vis spectrophotometer and spectroscopic ellipsometry. The hydrophilic properties of the films, after exposed to ultraviolet illumination, were analyzed from contact angle measurements. The results suggested that the substrate temperature at 300 °C was critical in the crystalline phase transformation from amorphous to anatase in the TiO_2 films. The obtained films exhibited good qualities in the optical properties, in addition to excellent photo-induced hydrophilic activities.

1. Introduction

Since the discovery of photo-induced splitting of water into H_2 and O_2 over titanium dioxide (TiO_2) electrode in 1972 [1], the research efforts in understanding the fundamental processes and in enhancing the photocatalytic efficiency of TiO_2 have drawn considerable attention [1–3]. It is well known that the main initial process for heterogeneous photocatalysis of organic and inorganic compounds is the generation of electron–hole pairs. When photons with energies greater than TiO_2 band gap (3.20 eV for anatase phase) are absorbed, electron–hole (e^-–h^+) pairs are created and migrate to the TiO_2 surface where they either recombine or participate in redox reactions with adsorbed species. It is generally believed that the holes oxidize water to hydroxyl radicals and generate electron reduction of oxygen to form superoxide anions. These radicals subsequently initiate a chain of reactions that oxidize the organic species into completion. The electron–hole pairs generated by absorption of a photon also play a fundamental role at the photo-induced superhydrophilicity [2–4]. While the electrons reduce Ti^{4+} cations to Ti^{3+}, the holes oxidize oxygen anions near the surface, thereby oxygen vacancies are created. These vacancies can be occupied by water molecules creating adsorbed OH groups. Thus the surface energy is minimized and the surface becomes hydrophilic. Proposed commercial products that exploit the photo-oxidative properties of TiO_2 films include self-cleaning glasses for automotive and architectural glass applications.

This work involves a development of TiO_2-based photocatalytic applications, which require an optimal preparation conditions for good-quality TiO_2 ultra-thin films. Because TiO_2 exists in three different crystalline forms, i.e., anatase (tetragonal), rutile (tetragonal), and brookite (orthorhombic), a formation of its phase depends on deposition method, starting material, and deposition temperature. Many methods for preparing the TiO_2 thin films include sol–gel coating [5,6], plasma enhanced chemical vapor deposition [6,7], electron-beam evaporation, [8] and magnetron sputtering [9–11]. Among them, a pulsed dc magnetron sputtering method is the most advantageous in controlling the structure and composition of the TiO_2 thin films due to its easiness to adjust deposition

* Corresponding author. Fax: +66 2872 5254.
E-mail address: mati.horprathum@nectec.or.th (M. Horprathum).

0925-8388/$ – see front matter.
doi:10.1016/j.jallcom.2011.01.038

condition. In addition, this method can be adapted to a large-area coating for industrial purposes.

Because the cost of film coating is directly proportional to the film thickness and the deposition temperature, the TiO_2 ultra-thin film deposited at minimum temperature is preferable in order to minimize the manufacturing cost. However, most of recent research reports have shown the effective hydrophilic and photocatalytic properties of TiO_2 films with thickness larger than 50 nm [12–14], only few groups demonstrated the photo-induced hydrophilic properties of TiO_2 ultra-thin films with thickness less than 15 nm. Sirghi and Hatanaka [15] reported that amorphous TiO_2 with thickness less than 12 nm could show hydrophilic properties. Glöß et al. [16] reported easy-to-clean or a self-cleaning properties achieved by deposited photocatalytic 10 nm thick TiO_2 as a top layer of an AR system on glass and polymer substrate. To take into consideration of the deposition temperature, the aim of this work is therefore to prepare and study the influence of substrate temperature (T_s) on the structural, optical and hydrophilic properties of TiO_2 ultra-thin films, at thickness of 15 nm, grown by pulsed dc reactive magnetron sputtering technique.

2. Experiments

2.1. Sample preparation

The TiO_2 ultra-thin films were prepared by a commercial pulsed dc reactive magnetron sputtering in both high purity argon (99.999%) and oxygen (99.999%) UHV system (AJA International, Inc.; ATC 2000-F) at a fixed deposition time of 15 min. A pulsed frequency of 20 kHz was used on a Ti (99.995%; KJ. Lesker) target of 2 in. diameter. The distance between a substrate holder and a titanium target was 90 mm, and the inclined angle of the sputtering gun was 40° with respect to the plane of substrate holder. The chamber was evacuated by mechanical pump (ALCATEL) and turbo-pump (Shimazu; TMP-803-LM). The base pressure of the deposition chamber was about 1×10^{-7} Torr. The operating pressure was 3 mTorr from a pressure-controlled gate valve. The gas flows of argon and oxygen were set at 10 and 20 sccm, respectively. The discharge was generated with a 400 W pulsed DC power. Substrates, i.e., glass slides and silicon wafers (1 0 0), were previously prepared by ultrasonic washer in acetone and isopropanol, successively, and then dried in nitrogen atmosphere before being loaded into the deposition chamber. Prior to the deposition, the substrates were cleaned by argon plasma ion at 5 mTorr for 5 min in order to remove surface contaminants. The titanium target was also pre-sputtered in an argon atmosphere at 5 mTorr in order to remove its oxide layer surface. The removal of oxide was immediately observed from a sudden change in discharged characteristics and a discharged color from a pale pink to blue. For the purpose of this experiment, the substrate temperature was selected as a variable parameter from 100 to 400 °C, as controlled and stabilized by a quartz halogen lamp for 15 min before, and during, the deposition.

2.2. Film characterization

The structure of the TiO_2 ultra-thin films was characterized by grazing-incidence X-ray diffraction (GIXRD; Rigaku Ttrax III). The Cu Kα radiation was operated at 50 kV, 300 mA with scanning speed of 2° per minute at 2θ step of 0.02°. The surface morphologies of the TiO_2 ultra-thin films were investigated by high resolution transmission electron microscopy (TEM; JEOL JEM-2010), and atomic force microscopy (Seiko, SPA 400) in a dynamic mode.

The optical characteristics of the obtained films were also analyzed. Light transmission of the films was characterized by a double-beam ultraviolet–visible light (UV–vis) spectrophotometer (PerkinElmer; Lambda 900). The measurements were conducted for spectral range of 250–860 nm. Several optical parameters, i.e., index of refraction, extinction coefficients, and film thicknesses, were calculated from ellipsometric technique using a variable-angle spectroscopic ellipsometer (VASE; J.A. Woollam) measured at 70° incident angles in the photon energy range of 1–6 eV.

The hydrophilicity was evaluated by a water contact angle measurement (ramé-hart instrument; model 250), which was performed in ambient air (i.e., 25 °C, relative humidity (RH) 50%). The UV-A illumination was carried out by a black light lamp with a power density of 1.2 mW/cm^2 and the maximum intensity center at 365 nm.

3. Results and discussion

3.1. Grazing-incidence X-ray diffraction

Fig. 1 shows GIXRD patterns of TiO_2 ultra-thin films deposited at different substrate temperatures. The structural characteristics of these films were hardly observed because of a very low-intensity of X-ray signals. This is a result of small X-ray scattering due to the ultra-thin structure. In spite of this fact, we recognized a low-intensity diffraction A (1 0 1) from the anatase phase of the films deposited at 300 °C (T_s). Nevertheless, no XRD response from the film deposited at 100–200 °C (T_s) was observed.

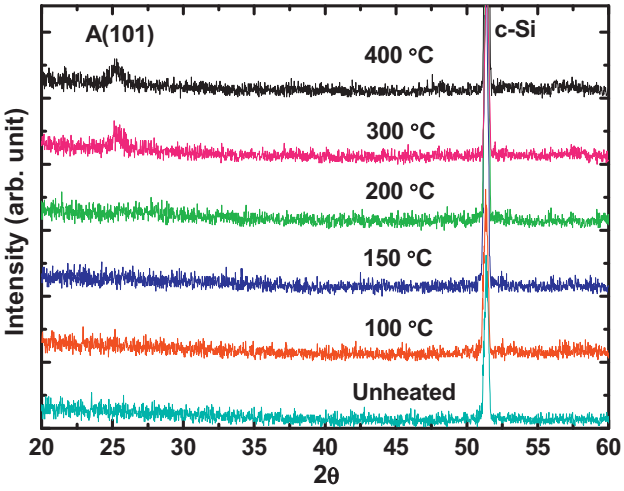

Fig. 1. GIXRD patterns of TiO_2 ultra-thin films deposited at room temperature up to 400 °C.

3.2. High resolution transmission electron microscopy (HRTEM)

The development of the microstructure in the direction of layer growth was additionally investigated on HRTEM cross-sections. Fig. 2(a) and (b) shows the comparison of HRTEM bright field images between the TiO_2 layer deposited at room temperature and at T_s = 400 °C, respectively. Fig. 2(a) reveals a completely amorphous layer of the film, while Fig. 2(b) reveals nano-crystalline traces. In addition, we noticed a homogeneous HRTEM contrast in all TiO_2 layer. The difference in the growth structure between room temperature and T_s = 400 °C confirms the results of the GIXRD measurements.

3.3. Surface roughness

Fig. 3 shows 2D AFM images of the TiO_2 ultra-thin films deposited on the Si (1 0 0) substrates at different substrate temperatures. From Fig. 3(a), without external heating, the surface morphology of the TiO_2 ultra-thin films deposited at room temperature was very smooth with roughness of 0.19 nm. When the substrate temperature was increased, the surface roughness was also increased. From Fig. 3(b), at 400 °C, the surface roughness was 0.37 nm. The increase in the surface roughness according to the substrate temperature during the film deposition could be explained from an effect of grain size growth.

3.4. Optical properties

First, the optical properties of the obtained films were analyzed from the transmittance percentage. Fig. 4 shows the UV–vis spectra of the TiO_2 ultra-thin films deposited at different substrate temperatures. When the substrate temperature was increased, the transmittance of the films was slightly decreased. The films deposited at higher temperatures were more absorbing due to insufficient oxygen incorporation in the film content during the deposition. With the increased substrate temperature, the condensation of oxygen was also decreased [17,18].

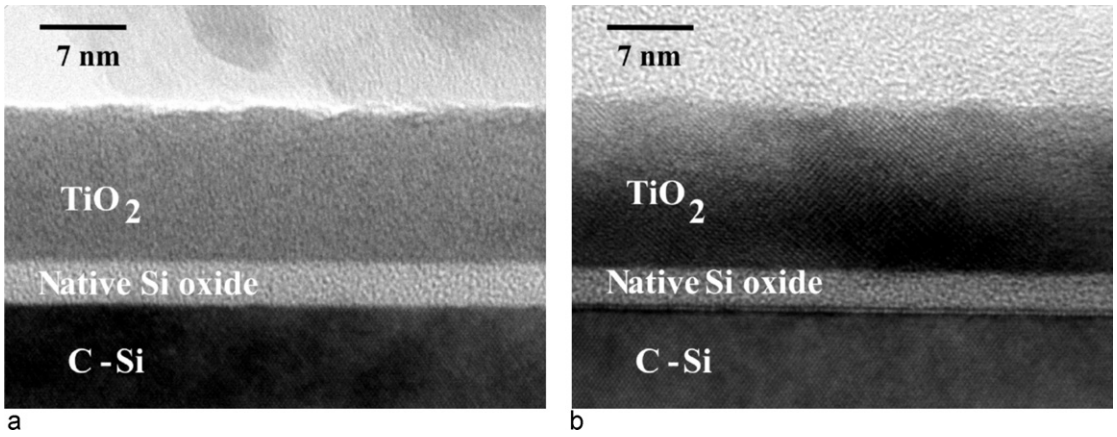

Fig. 2. Cross-sectional HRTEM images showing the crystallinity of TiO_2 ultra-thin films deposited at (a) room temperature and (b) T_s = 400 °C.

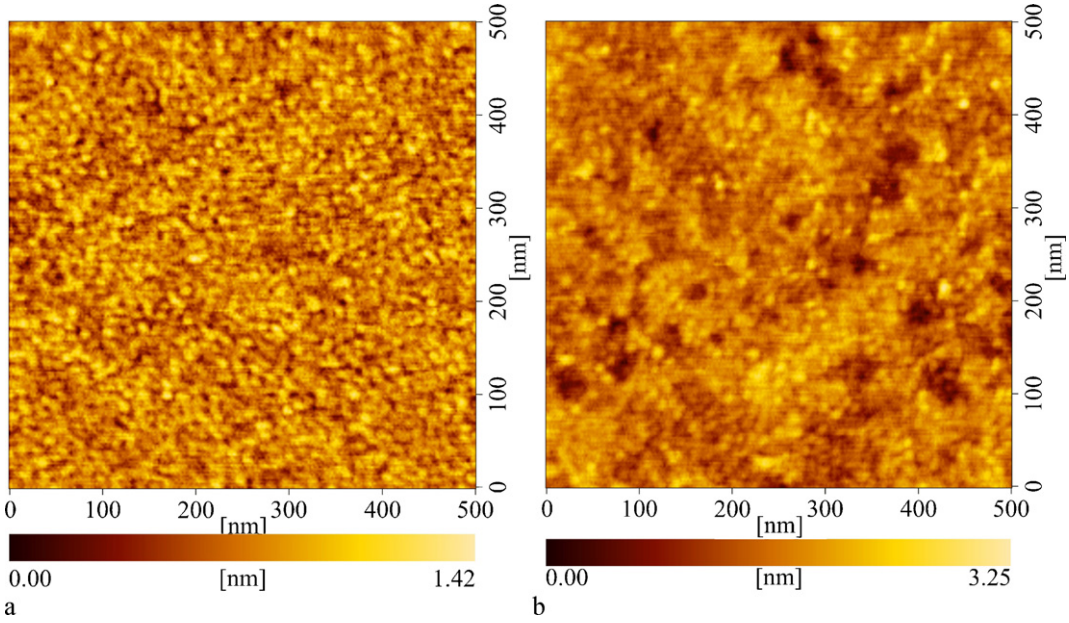

Fig. 3. AFM images of TiO_2 ultra-thin films deposited at (a) room temperature and (b) T_s = 400 °C.

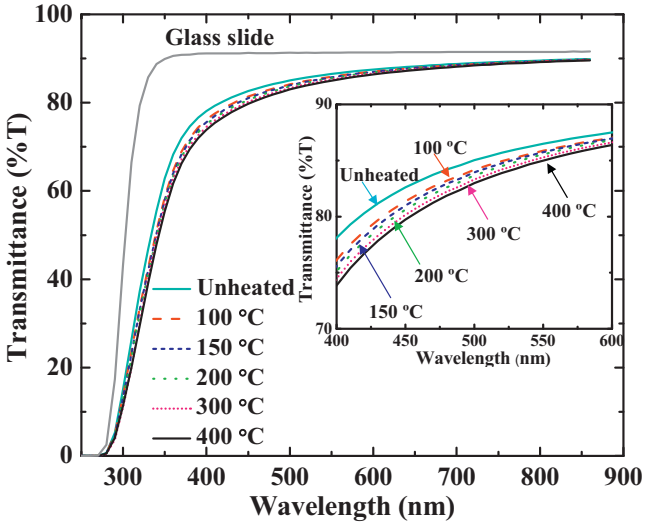

Fig. 4. Transmittance spectra as a function of wavelength for TiO_2 ultra-thin films deposited at different substrate temperatures.

Next, film thickness, refractive index (n) and extinction coefficient (k) of a transparent film were characterized by spectroscopic ellipsometry (SE) [19]. In the SE analyses, a single-layer model (TiO_2 layer/native SiO_2/substrate) was used as we assumed homogeneity and ignored the film's surface roughness. An interfacial layer native silicon dioxide, assumed at 2 nm thick, was included because the Si substrates were not etched by HF before the film deposition. This structural model has been confirmed by cross-section HRTEM micrograph as shown in Fig. 2, where the 15 nm TiO_2 layer on top of approximately 3 nm thick native Si oxide layer was clearly observed. With such physical model, the Cody-Lorentz oscillator was used to represent the optical dispersion model. The Cody-Lorentz oscillator enabled us to deduce optical band gap and exploit band-to-band transition regions between the band edge and the Urbach tail [8,20–22].

The dependences of n and k on the variation of the substrate temperature with varied photon energy are presented in Fig. 5. The films deposited without an external heating showed refractive index (n at 550 nm) of 2.36, which was increased to 2.50 for films deposited at T_s = 300 °C. The increase in the refractive index of the films deposited at higher temperature was a result of the increase in packing density and crystallinity [23]. Both ellipsometric analysis and XRD have confirmed these results.

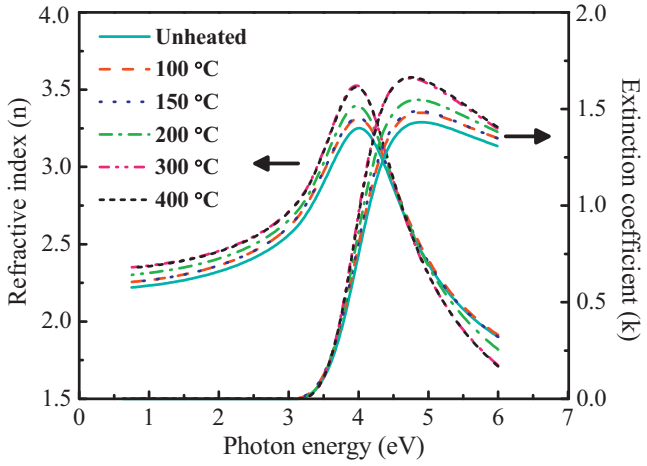

Fig. 5. The variation of optical constants as a function of photon energy of TiO_2 ultra-thin films deposited at different substrate temperatures.

The packing density of the films could be explained by Clausius–Mossotti relation [24,25]. The relation between the packing density (P), defined as the ratio of the film density (ρ_f) to the bulk density (ρ_b) of the material and the corresponding refractive index of the material was given in Eq. (1) [25,26]

$$P = \left(\frac{\rho_f}{\rho_b}\right) = \left(\frac{n_f^2 - 1}{n_f^2 + 2}\right)\left(\frac{n_b^2 + 2}{n_b^2 - 1}\right) \quad (1)$$

where n_f and n_b were the refractive index of the film and the bulk material of TiO_2, respectively. In the present study, the refractivity of bulk anatase TiO_2 (n_b) was 2.52 [27]. The ρ_f and ρ_b were the density of the film and bulk material, respectively. The packing density of the films was calculated from the refractive index values. Fig. 6 shows the variation of packing density of TiO_2 ultra-thin films as a function of substrate temperature. It can be seen that the packing density of the films was gradually increased upon the increase in the substrate temperature. This result indicated that the TiO_2 films became denser as the deposited temperatures were increased.

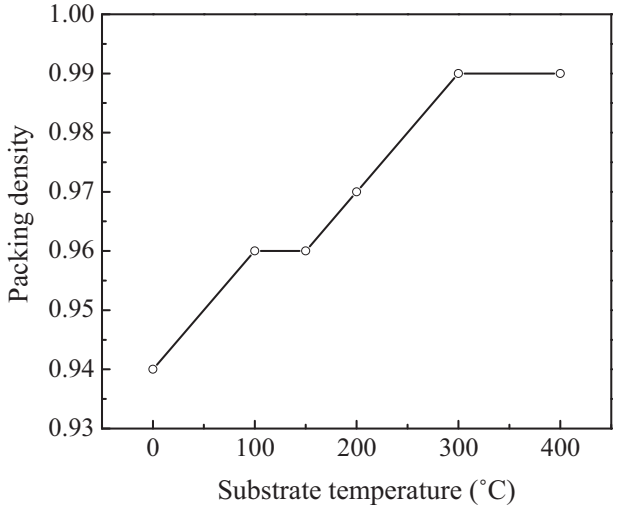

Fig. 6. Variation of packing density of TiO_2 ultra-thin films deposited at different substrate temperatures.

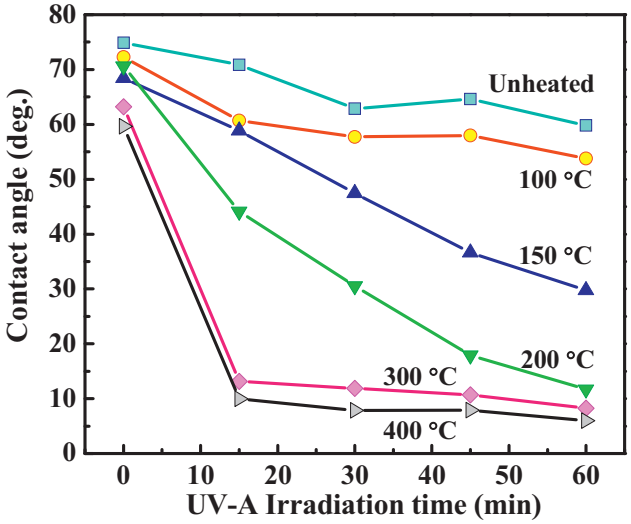

Fig. 7. Water contact angle variation following the UV illumination time for the TiO_2 ultra-thin films deposited at different substrate temperatures.

3.5. Photo-induced hydrophilic properties

The hydrophilicity of the deposited films was investigated by measurements of the water contact angles. Fig. 7 shows the change in the contact angle as a function of the UV-A illumination time on the TiO_2 ultra-thin films deposited at different substrate temperatures. When the film surface was illuminated by UV-A light, water contact angle started to decrease, indicating an increase in the photo-induced hydrophilicity. The TiO_2 ultra-thin films deposited without an external substrate heating and $T_s = 100\,^{\circ}C$ did not show a significant photo-induced hydrophilicity. When the deposition temperature was increased to 300 and 400 °C, the water contact angles were smaller at approximately 6° after 1 h of irradiation. These results indicated excellent photo-induced hydrophilicity of these films. The difference in photo-induced hydrophilicity could be interpreted from the difference in physical properties between amorphous and anatase phase within the content of the films. It has been reported that anatase crystallinity of the TiO_2 films easily formed oxygen vacancies on the surface, thus resulting in photo-induced hydrophilic properties [28].

4. Conclusions

The pulsed dc reactive magnetron sputtering method was used to prepare the TiO_2 ultra-thin films at several substrate temperatures. The structural properties of the 15 nm thick TiO_2 films have been successfully characterized by GIXRD and HRTEM. The substrate temperature was found to have a significant effect on the structural and photo-induced hydrophilic properties. With the substrate temperature up to 200 °C, the obtained films were all amorphous. When the substrate temperature was increased to 300 °C, the TiO_2 films showed the anatase phase structure. Corresponding to the crystalline phase change, the SE analyses showed that the refractive index of the TiO_2 ultra-thin film was also increased with the increase in the substrate temperature. Such results were closely related to insufficient oxygen incorporation and the packing density in the deposited films. The experiments indicated that the substrate temperature of 300 °C was critical for higher packing density within the TiO_2 films. Moreover, the photo-induced hydrophilic showed a clear tendency to increase with the increased substrate temperature. In this study, the TiO_2 ultra-thin films with thickness of 15 nm, when deposited at 300 °C, held promising photo-induced hydrophilic activities, which could be

utilized in several applications, i.e., self-cleaning and anti-fogging glasses.

Acknowledgments

This work was supported by the National Electronics and Computer Technology Center (NECTEC) and the National Research University. The author would like to thank Mr. Alongkot Treetong (NANOTEC) for his help in AFM measurement.

References

[1] A. Fujishima, K. Honda, Nature 238 (1972) 37–38.
[2] A. Fujishima, T.N. Rao, A. Tryk, J. Photochem. Photobiol. C: Photochem. Rev. 1 (2001) 1–21.
[3] O. Carp, C.L. Huisman, A. Reller, Prog. Solid State Chem. 32 (2004) 33–177.
[4] R. Wang, K. Hashimoto, A. Fujishima, M. Chikuni, E. Kojima, A. Kitamura, M. Shimohigoshi, T. Watanabe, Nature 388 (1997) 431–432.
[5] A. Nakajima, A. Nakamura, N. Arimitsu, Y. Kameshima, K. Okada, Thin Solid Films 16 (2008) 6392–6397.
[6] C. Guillard, D. Debayle, A. Gagnaire, H. Jaffrezic, J.M. Herrmann, Mater. Res. Bull. 39 (2004) 1445–1458.
[7] H. Szymanowski, A.S. Guzenda, A. Rylski, W. Jakubowski, M.G. Lipman, U. Herberth, F. Olcaytug, Thin Solid Films 515 (2007) 5275–5281.
[8] P. Eiamchai, P. Chindaudom, A. Pokaipisit, P. Limsuwan, Curr. Appl. Phys. 9 (2009) 707–712.
[9] K. Eufinger, E.N. Janssen, H. Poelman, D. Poelman, R. De Gryse, G.B. Marin, Thin Solid Films 515 (2006) 425–429.
[10] Y. Zhang, X. Ma, P. Chen, D. Yang, J. Cryst. Growth 300 (2007) 551–554.
[11] M. Horprathum, P. Chindaudom, V. Patthanasettakul, S. Rotbuathong, P. Eiamchai, P. Limsuwan, Adv. Mater. Res. 55–57 (2008) 441–444.
[12] D. Glöß, P. Franch, O. Zywitzki, T. Modes, S. Klinkenberg, C. Gottfried, Surf. Coat. Technol. 200 (2005) 967–971.
[13] K. Eufinger, D. Poelman, H. Poelman, R. De Gryse, G.B. Marin, Appl. Surf. Sci. 254 (2007) 148–152.
[14] Q. Ye, P.Y. Liu, Z.F. Tang, L. Zhai, Vacuum 81 (2007) 627–631.
[15] L. Sirghi, Y. Hatanaka, Surf. Sci. Lett. 530 (2003) L323–L327.
[16] D. Glöß, P. Franch, C. Gottfried, S. Klinkenberg, J.S. Liebig, W. Hentsch, H. Liepack, M. Krug, Thin Solid Films 516 (2008) 4487–4489.
[17] E. Ritter, J. Vac. Sci. Technol. 6 (1966) 225–226.
[18] H. Kuster, J. Ebert, Thin Solid Films 70 (1980) 43–47.
[19] P. Chindaudom, K. Vedam, Appl. Opt. 33 (1994) 2664–2671.
[20] J. Price, P.Y. Hung, T. Rhoad, B. Foran, Appl. Phys. Lett. 85 (2004) 1701–1703.
[21] A.S. Ferlauto, G.M. Ferreira, J.M. Pearce, C.R. Wronski, R.W. Collins, X. Deng, G. Ganguly, Thin Solid Films 455–456 (2004) 388–392.
[22] M. Horprathum, P. Chindaudom, P. Limsuwan, Chin. Phys. Lett. 24 (2007) 1505–1508.
[23] M.H. Suhail, G.M. Rao, S. Mohan, J. Appl. Phys. 71 (1992) 1421–1427.
[24] C. Kittel, Solid State Physics, John Wiley & Sons, New York, 1971.
[25] W. Heitman, Thin Solid Films 5 (1970) 61–67.
[26] C.R. Ottermann, K. Bange, Thin Solid Films 286 (1996) 32–34.
[27] W.D. Kingery, H.K. Bowen, D.R. Uhlman, Introduction to Ceramics, Wiley, New York, 1976.
[28] R. Wang, N. Sakai, A. Fujishima, T. Watanabe, K. Hashimoto, J. Phys. Chem. B 103 (1999) 2188–2194.